

Modeling of Band-to-Band Tunneling Mechanisms

W. Bergner and R. Kircher

Siemens AG, Corporate Research and Development
Silicon Process Technology (SPT 33)
Otto-Hahn-Ring 6, 8000 Munich 83, FRG

Measurements and simulations are presented, which allow a better understanding of leakage mechanisms in reverse biased gated diodes. The model for the device simulation uses two mechanisms. In the high field regime the leakage current is identified as direct band-to-band tunneling. In the low field regime it is described as surface-state enhanced tunneling, which combines thermal activation of an electron to a surface-state and tunneling.

1. Introduction

Isolation structures often exhibit a parasitic gated diode when a thin oxide separates a charged electrode from a p-n junction. One example for this is a trench which cuts a well boundary, another one the gate-drain overlap of a MOS transistor. Such a structure as shown in Fig. 1 represents a critical leakage source in integrated circuits.

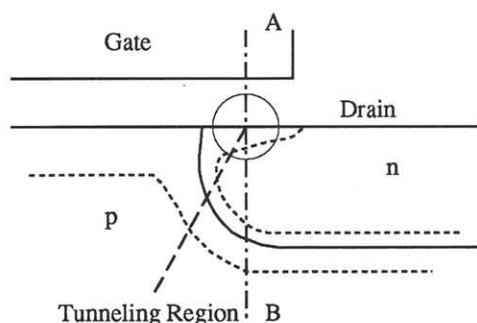


Figure 1: Gated diode structure

In addition to the well known enhancement of the diode saturation current, resulting from surface generation of the reverse biased p-n junction, an exponentially increasing current is observed (for

measurements see Fig. 3 and 5). Although the leakage current for high accumulation can be identified as band-to-band tunneling from its weak temperature dependence, a direct tunneling mechanism can not correctly describe the transition to the low field regime¹⁾. This leakage current exhibits three characteristic features: Firstly, the current depends exponentially on the reverse bias of the junction as well as on the gate voltage and can not be explained by a simple thermal generation model. Secondly, it does not vanish in the low field region, where the band bending inhibits direct band-to-band tunneling. And finally, the current has a strong temperature dependence which is not typical for tunneling currents.

2. Band-to-Band Tunneling

For high gate field strength the band bending in the gate-drain overlap region is sufficient for direct tunneling from the valence band to the conduction band. If we compare a typical tunneling length of about 100\AA with the curvature of the electric field lines, we see that the tunneling path and

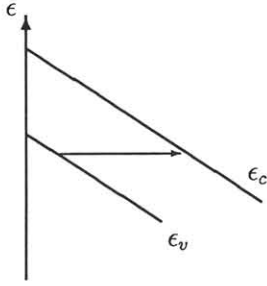


Figure 2: Band diagram along the cross section \overline{AB} for the case of direct band-to-band tunneling

the tunneling barrier can be described appropriately by one dimensional cuts through the potential distribution (Fig. 2). In this model we can take for the tunneling current

$$j_{vc} = Z \int_{\epsilon_v}^{\epsilon_c} d\epsilon \int_0^{\epsilon} d\epsilon_{\parallel} f_v(1 - f_c) T(\epsilon, \epsilon_{\parallel}).$$

The factor Z includes the density of tunneling states in the valence band as well as the probability of phonon scattering, which is necessary to overcome the indirect band gap in silicon. The Fermi-Dirac function f gives the occupation probability for an electron of energy level ϵ in the valence band f_v and the conduction band f_c , respectively. Whereas ϵ_{\parallel} denotes the energy of the incident electron parallel to the field.

For the implementation in the 2D device simulator GALENE II^{2,3)} we have utilized two different methods to calculate the tunneling probability T . First the WKB method gives

$$T = \exp[-2 \int k dx],$$

where k stands for the semiclassical momentum

$$k = \sqrt{\frac{2m^*}{\hbar^2} (\epsilon_{gap} - \epsilon - \epsilon_{parallel})}.$$

The integration over the barrier from the incident point to the end point can be done numerically using a solution of the device simulator to obtain the energy bands and the Fermi levels. Second it is possible to calculate the wave function from the one dimensional Schrödinger equation for a given potential distribution numerically with the Fox-Goodwin

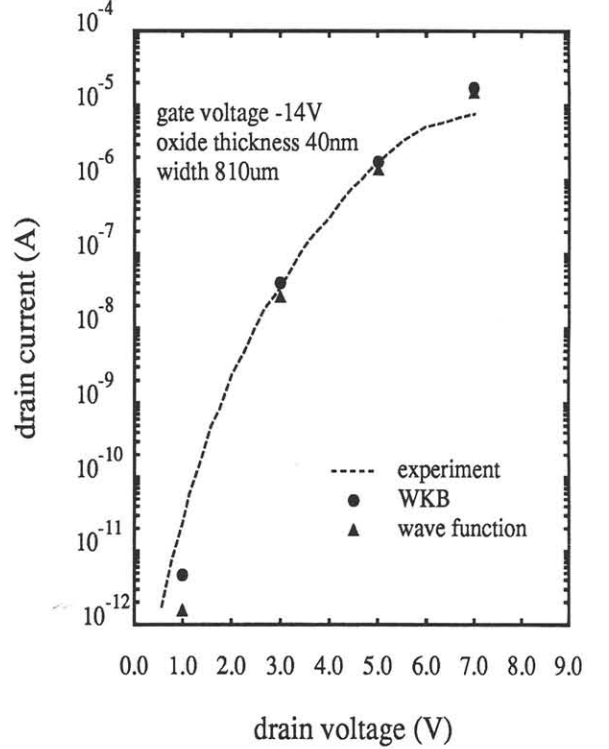


Figure 3: Comparison between experiment and simulation for the high field regime

algorithm⁴⁾. In this case the tunneling probability can be obtained from

$$T = \left| \frac{\Psi_e}{\Psi_i} \right|^2,$$

the ratio between the tunneling and the incident wave function. Fig. 3 compares both methods with experimental data. The close agreement between the two models shows that WKB is a good approximation for the tunneling probability.

3. Surface-State Enhanced Tunneling

To explain the leakage behavior in the low field regime for the case of deep electron depletion, we assume a two step mechanism as illustrated in Fig. 4. The first step consists of the thermal activation of an electron from the valence band to a surface-state in the band gap (I). There it sees a reduced barrier height. In the second step the electron tunnels through this reduced barrier to the conduction band (II). This mechanism is similar to the trap assisted tunneling in bulk silicon and can be expressed as

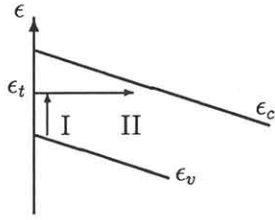


Figure 4: Band diagram along the cross section \overline{AB} for the low field case

surface generation term:

$$G_{vc} = E \cdot f_v (1 - f_c) \int_{\epsilon_v}^{\epsilon_c} D_t(\epsilon_t) T(\epsilon_t) \exp\left[-\frac{\epsilon_t - \epsilon_v}{U_{th}}\right] d\epsilon_t.$$

D_t represents the trap density in the bandgap and the Boltzmann factor stands for the thermal activation probability. The tunneling probability $T(\epsilon_t)$ through the reduced barrier is calculated with WKB approximation.

The model has been implemented in GALENE II selfconsistently, and contains only one scaling factor E , which is correlated with the emission coefficient from the surface. This factor is obtained by fitting the calculated current at one chosen bias condition to the measured value. The model for the trap density D_t is equivalent to the model for surface-states⁵⁾ used in several device simulators. As input for the evaluation of the new generation model, profiles from 2D process simulation have been used. Fig. 5 shows the excellent agreement between measured leakage currents and simulations with the new surface generation model.

Acknowledgement

We would like to greatly acknowledge Dr. Werner Weber for providing test devices and for valuable discussions.

References

- 1) W.P. Noble et al.; IEEE-ED **36** (1989) 720.
- 2) W.L. Engl et al.; VLSI Process/Device Modeling Workshop (1987), Tokyo.

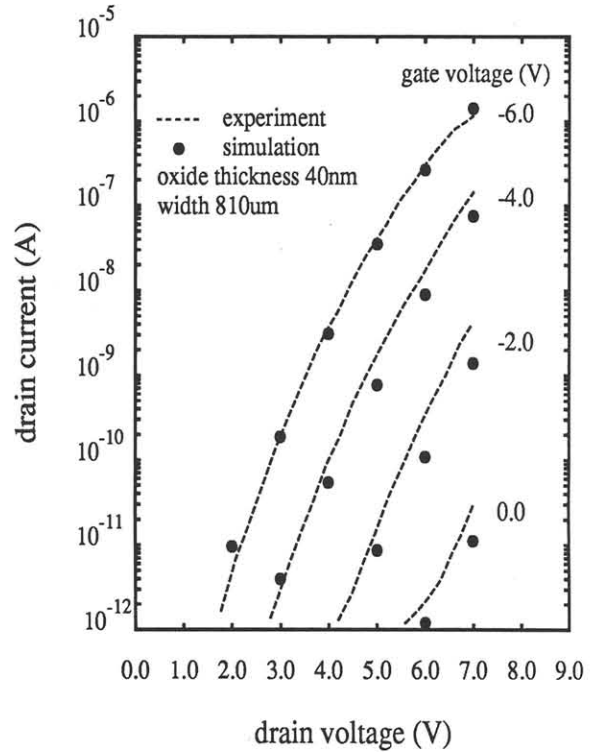


Figure 5: Comparison between experiment and simulation for the surface-state model

- 3) GALENE II User's Guide (1988). RWTH Aachen, West Germany.
- 4) L. Fox et al.; Proc. Camb. Phil. Soc. **45** (1949) 373.
- 5) A. Schwerin; IEEE-ED **34** (1987) 2493.

